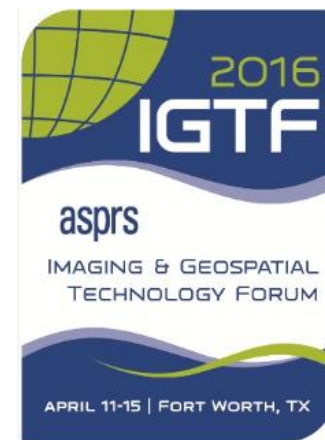


# Application Of The Specular Array Radiometric Calibration (SPARC) Method For The Vicarious Calibration Of Landsat Sensors

Raytheon Space and Airborne Systems  
Stephen J. Schiller

April 13, 2016  
Joint Agency Commercial Imagery  
Evaluation (JACIE) Workshop



# Introduction

---

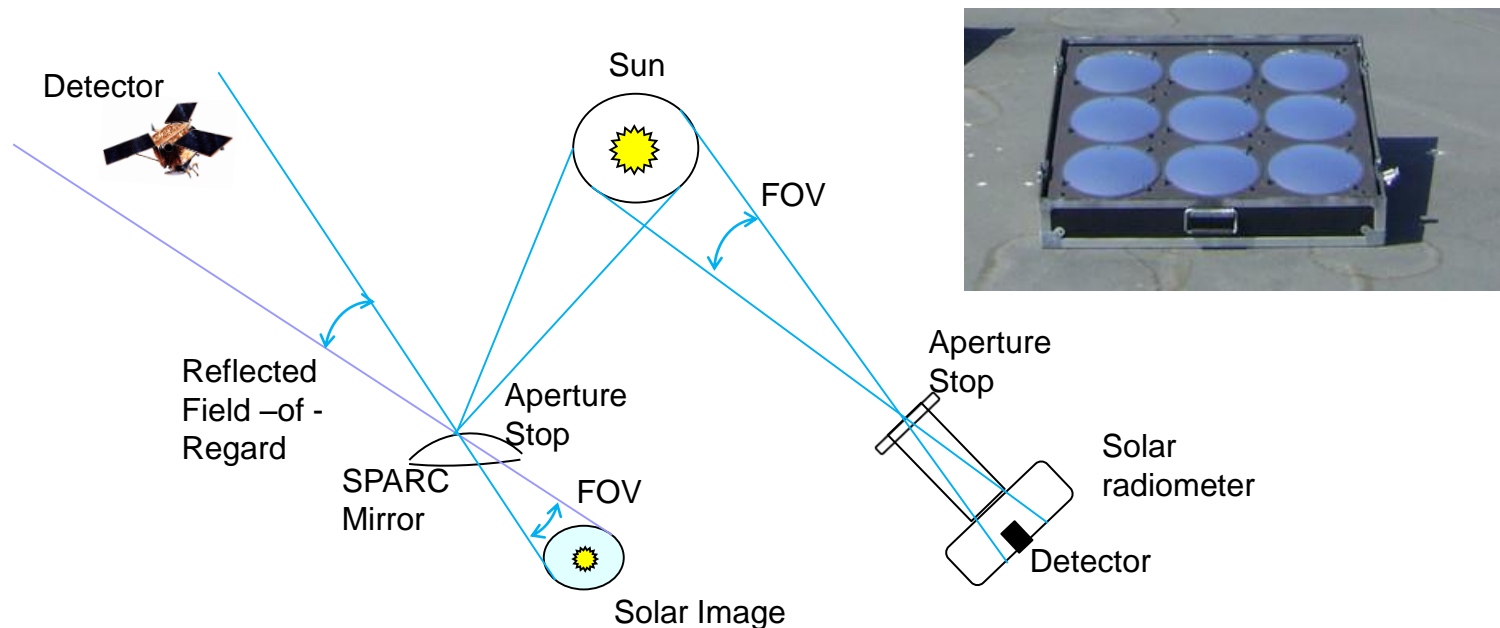
- Vicarious calibration has played an important role in the in-flight radiometric assessment of Landsat sensor systems for many years, principally to validate the absolute performance of the on-board calibrator.
- The effort to continue the Landsat heritage into the future through the Sustainable Land Imaging initiative, considers the potential to move vicarious methods into a more prominent calibration role potentially replacing on-board absolute calibration. The objective is to reduce cost and schedule through lower power, weight, and volume in future designs.
- This presentation describes a on-going effort to support this objective using Raytheon's Specular Array Radiometric Calibration (SPARC) method in a vicarious calibration study of Landsat 8.

Results presented are preliminary

- NASA support for this research is gratefully acknowledged through the NASA ROSES program grant No. NNX15AV43G.

# Conceptualizing The SPARC Method

The SPARC method allows any earth observing sensor to image the sun, just like a solar radiometer, and be calibrated directly to the solar spectral constant. The reflective Field-of-View for a mirror acts as a Field-of-View (FOV) aperture stop just as with an aperture stop on a typical sun photometer allowing the sun to be viewed directly as an absolute reference.



The mirror also acts as an ideal neutral density filter. By selecting an appropriate radius of curvature of the mirror, it scales down the brightness of the sun to an intensity that does not saturate the sensor focal plane and does so without changing upwelling spectral properties.

# SPARC Radiometric Calibration Capability Heritage

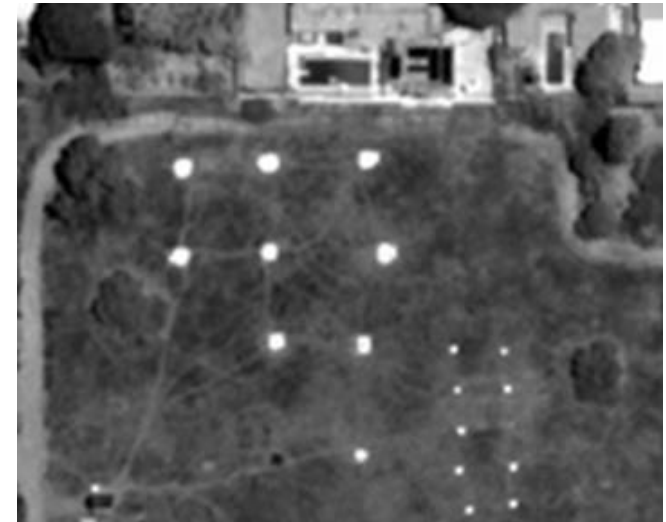
- Method has been demonstrated with IKONOS and Quickbird

IKONOS

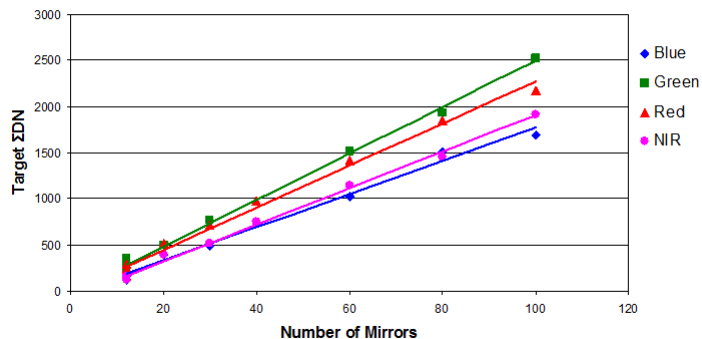


The SPARC method has been applied to small footprint sensors demonstrating its capability of providing accurate and repeatable radiometric references for calibration applications

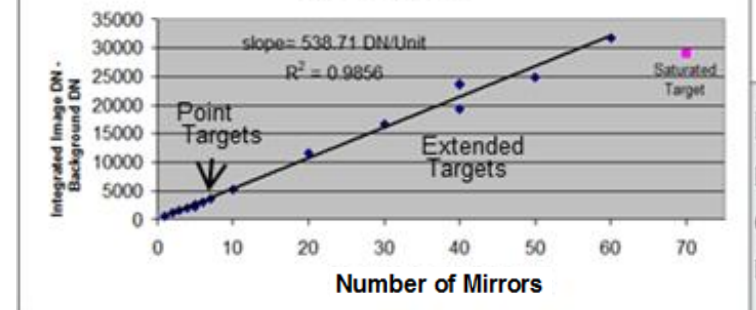
Quickbird



DN/Mirror: Image po\_365282 Glass Mirror SPARC Target



Quickbird Pan Band Linearity Response All Mirror Arrays



Plots demonstrate consistency in the radiometric response to SPARC targets over the sensor dynamic range.

# SPARC Absolute Radiative Transfer Equation

- The absolute radiometric calibration of a sensor proceeds from the SPARC radiative transfer equation.

## At-Sensor In Band Radiance/mirror For A SPARC Target

$$L_{at-sensor}(\lambda) / mirror = \rho(\lambda)\tau_{\downarrow}(\lambda)\tau_{\uparrow}(\lambda)E_o(\lambda)\left(\frac{R}{2GSD}\right)^2$$

Watts/(m<sup>2</sup> sr micron)

$\rho(\lambda, \theta_r)$  = Mirror specular reflectance  
 $\tau_{\downarrow}(\lambda)$  = Sun to ground transmittance  
 $\tau_{\uparrow}(\lambda)$  = Ground to sensor transmittance

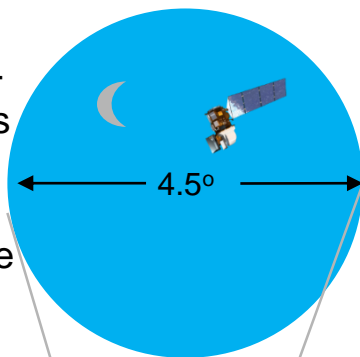
$E_o(\lambda)$  = Solar spectral constant  
 $R$  = Mirror radius of curvature (m)  
 $GSD$  = Ground sample distance normal to line-of-sight (m)

- The radiance is the total integrated energy reaching the sensor within a SPARC target image profile
- The goal is to compare the vicarious SPARC predicted radiance to the sensor radiance reported in the Landsat 8 L1R calibrated imagery for individual targets

# Landsat SPARC Target Design

Because SPARC targets are specular intensity sources and Landsat has a large GSD, the mirror radius of curvature is much larger than used commercial sensors to produce the same effective radiance.

The reflected field-of-regard produces a uniform illumination intensity across the sky = 4.5 degrees



## SPARC Calibration Panels:

- Four 18" diameter mirrors on each telescope mount (9 lbs each)
- 10 m Radius of curvature mirrors
- Clear Field-of-Regard (FOR) = 4.5°
- Deployed on a portable iOptron® iEQ45 ProTM alt-az telescope mount.
- Built-in 32-channel Global Positioning System (GPS).
- Payload mirror assembly on each mount is about 50 lbs
- Four deployable panels (each on separate mounts) are used to provide up to 3 calibration radiance levels in a single Landsat image collect.

# Mirror Construction

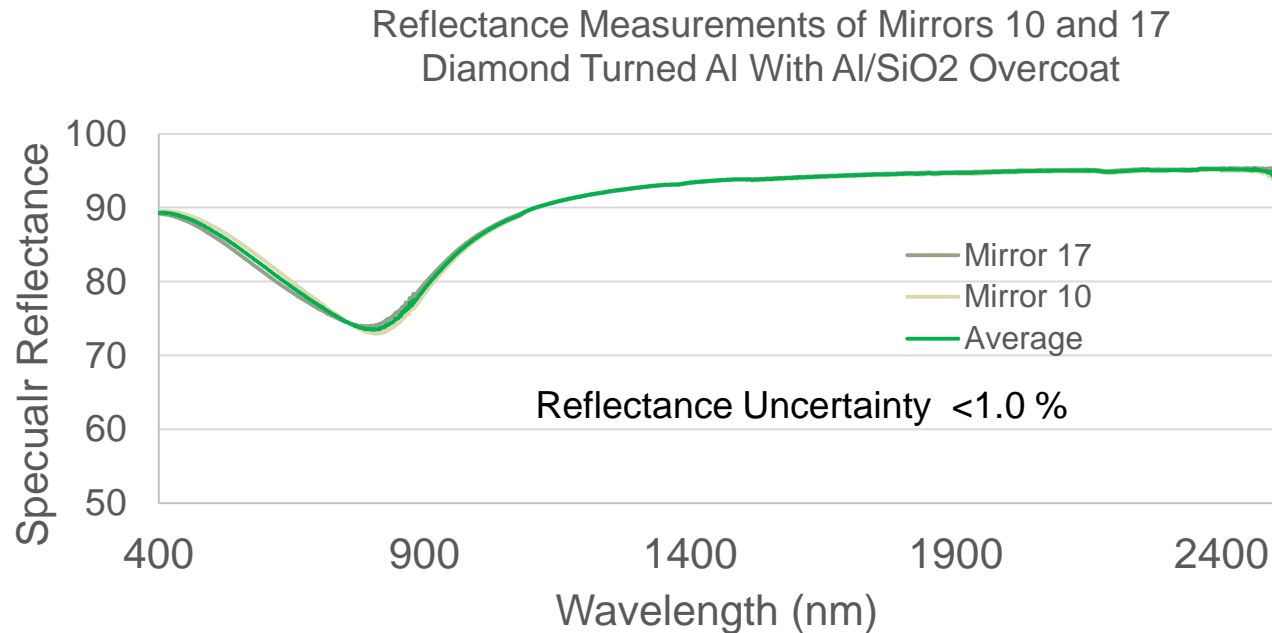
- Diamond turned convex spherical mirrors
- Radius of curvature = 10 m +/- 0.1%
- Clear convex surface diameter = 18.0 inches



A Mirror radius of curvature is selected to create a target producing an at-sensor radiance response equivalent to a 80% Lambertian surface based on 12 mirrors at 30 m GSD.

# Mirror Reflectance Measurements

Mirror witness samples were measured in the Raytheon Optical Materials Measurements Laboratory with a Perkin Elmer reflectometer.



	Band Integrated Reflectance							
	CA	Blue	Green	Red	NIR	SWIR1	SWIR2	Pan
Band Center (nm)	442.9	482	561.4	654.6	864.7	1608.9	2200.7	589.5
Reflectance	88.82	87.56	83.96	79.04	76.16	94.08	94.99	82.33

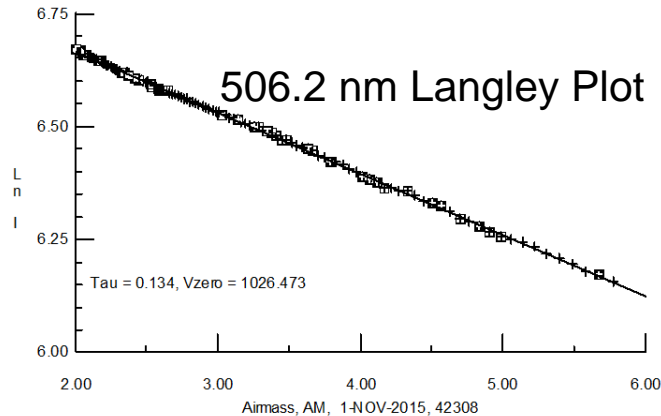
# SPARC Radiometric Target Designed For Landsat 30 m Multispectral Calibration



Portable system provides computer controlled pointing with sub-arcminute resolution and potential satellite tracking capability

# Seven Band Shadow Band Radiometer for Measuring Atmospheric Transmittance

The atmospheric transmittance at each overpass is measured using a seven channel shadowband radiometer. Measurement is every 15 seconds, averaged to 1 minute intervals.



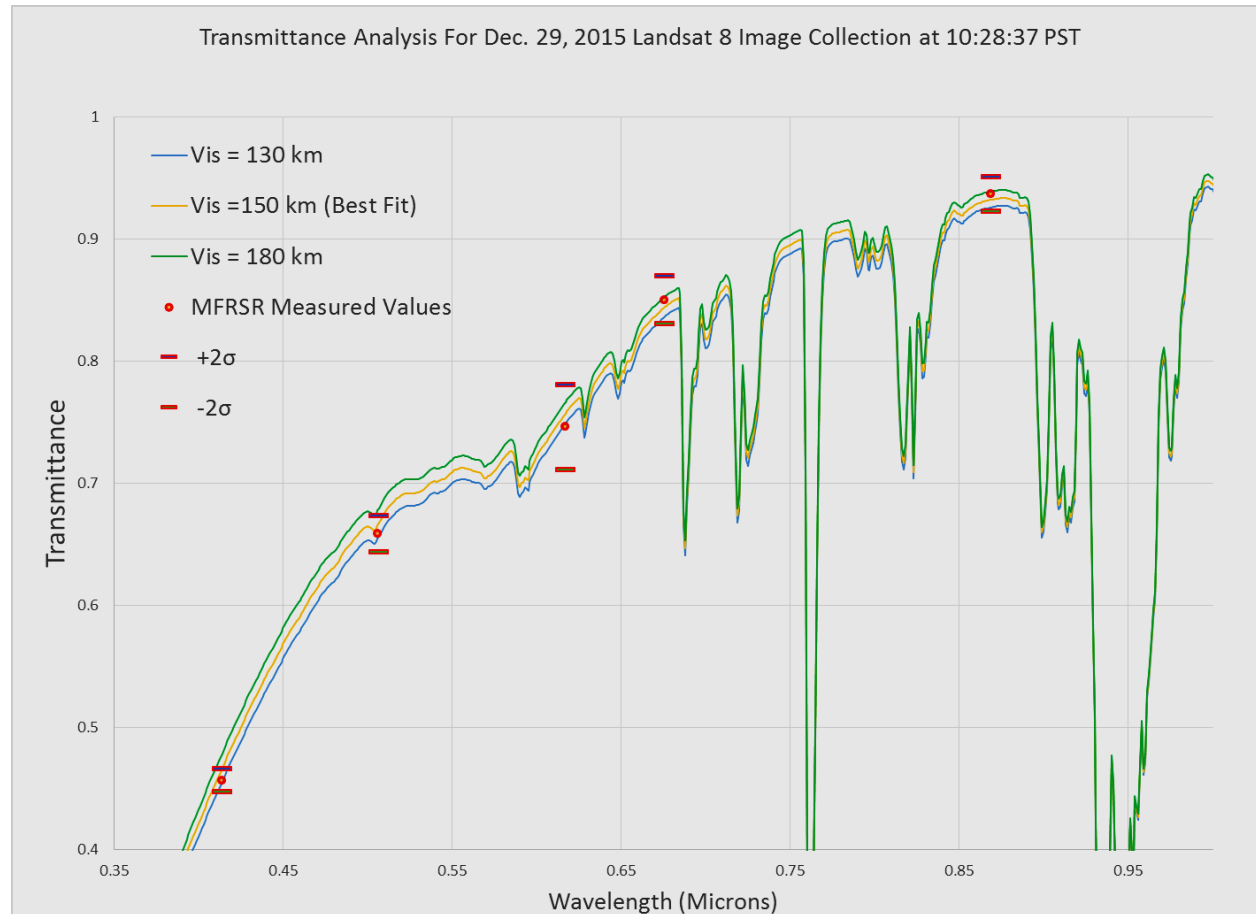
Calibrated using the Langlely plot method from data collected at Table Mountain Observatory (7500 ft) over 5 weeks in Oct. and Nov. 2015

Top-of-atmosphere irradiance calibration coefficients based on 28 morning and afternoon Langlely plots

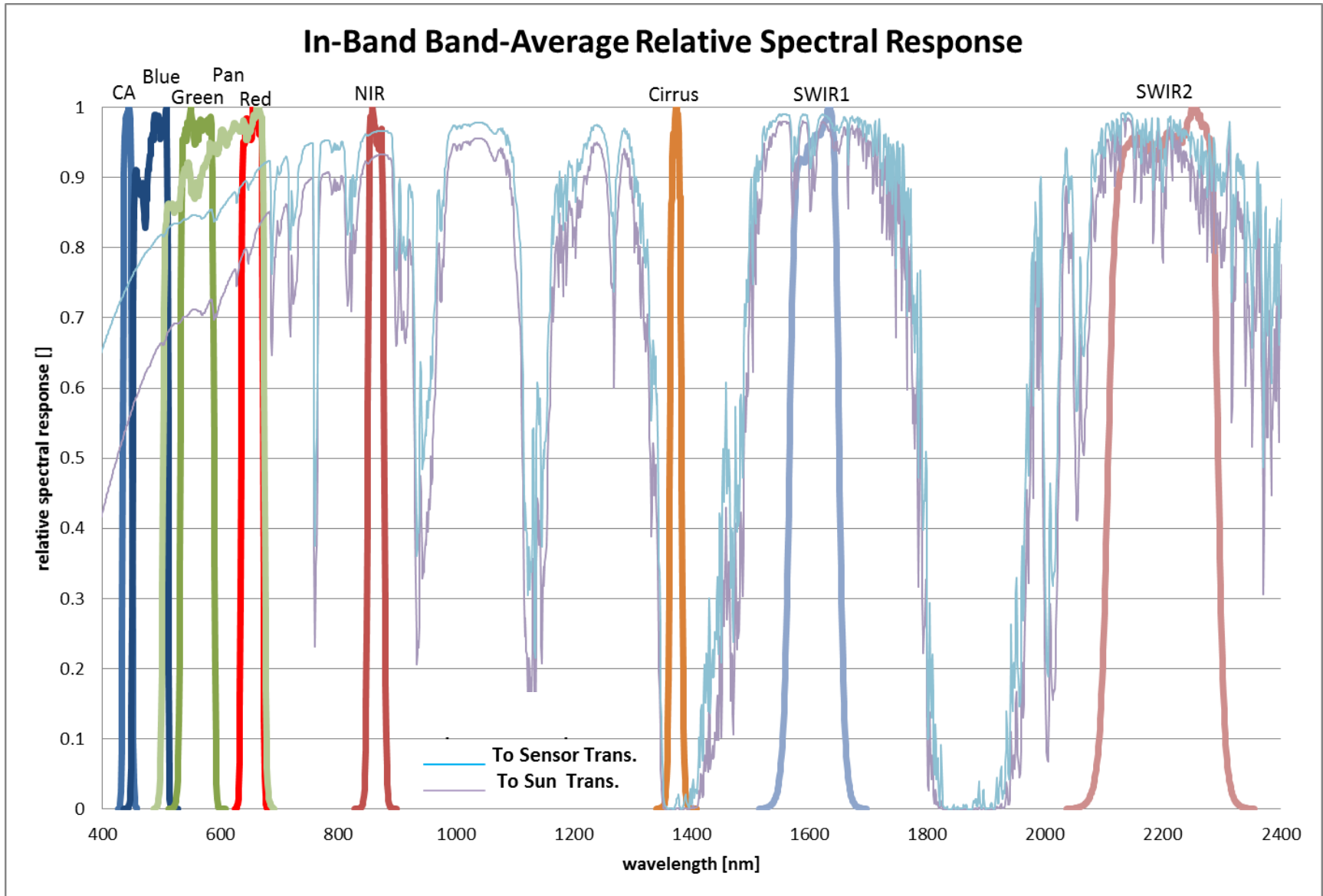
Wavelength (nm)	413.9	506.2	616.8	675.5	868.5
$I_o$ Average (1 AU)	1370.708	996.7491	305.9666	543.4447	1885.081
Std Dev.	14.403	11.415	7.111	6.199	14.163
%Error	1.051	1.145	2.324	1.141	0.751

# MODTRAN Model Fit To Transmittance Measurements

The sun-to-ground transmittance measured by shadowband radiometers provide input parameters for constraining a MODTRAN Radiative transfer model to calculate the Landsat in-band transmittance at the time of the overpass



# MODTRAN Model Spectrum Is Integrated With Band Spectral Response To Determine In-band Transmittance



# Calculation Of Vicarious Predicted At-Sensor Radiance Of SPARC Targets For the Feb. 15 Overpass

$$L_{at-sensor}(\lambda) / mirror = \rho(\lambda)\tau_{\downarrow}(\lambda)\tau_{\uparrow}(\lambda)E_o(\lambda)\left(\frac{R}{2GSD}\right)^2$$

$E_o(\lambda)$  = Modtran CHKUR In-band TOA Solar Irradiance

$R = 10\text{ m}$  and  $GSD = 28.8\text{ m}$  (measured from L1R image product)

L8 Band	CA	Blue	Green	Red	NIR	SWIR1	SWIR2	Pan
Band Center (nm)	442.9	482	561.4	654.6	864.7	1608.9	2200.7	589.5
Reflectance	0.8882	0.8756	0.8396	0.7904	0.7616	0.9408	0.9499	0.8233
To Sun Trans	0.6512	0.7265	0.7907	0.8739	0.9668	0.9646	0.9413	0.8160
To Sensor Trans	0.7685	0.8218	0.8656	0.9204	0.9795	0.9766	0.9618	0.8823
$E_o$ (W/m <sup>2</sup> um)	1888	1975	1852	1570	951.2	242.4	82.49	1751
Radiance /mirror (W/m <sup>2</sup> *str*um)	25.30	31.12	32.08	30.09	20.68	6.48	2.14	31.28
8 mirrors (W/m <sup>2</sup> *str*um)	202.37	248.95	256.63	240.68	165.43	51.80	17.11	250.25

# Uncertainty In A Single SPARC Target Vicarious At-Sensor Radiance Prediction

Based the gain equation, the RSS uncertainty in the at-sensor radiance of a single SPARC target reference is (assuming clear sky conditions)

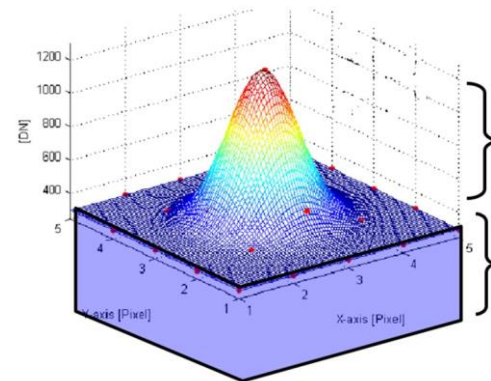
$$\frac{\delta L}{L}(SPARC) = \sqrt{\left(\frac{\delta\rho}{\rho}\right)^2 + \left(2 * \frac{\delta\tau}{\tau}\right)^2 + \left(\frac{\delta E_o}{E_o}\right)^2 + \left(2 * \frac{\delta R}{R}\right)^2 + \left(2 * \frac{\delta GSD}{GSD}\right)^2}$$

Symbol	Parameter	% Uncertainty
$\rho$	Mirror Reflectance	1.0%
$\tau_{\downarrow}, \tau_{\uparrow}$	Measured and Modeled Atmospheric Trans. (applied as correlated)	1.5%
$E_o$	In-band Top-of- Atmosphere Solar Irradiance	2.0% Abs., 0.2% Rel
$R$	Mirror Radius of Curvature	0.1%
$GSD$	Pixel Projected Ground Sample Distance	1.0%
$L$	Absolute At-Sensor Radiance	RSS total = 4.3% Abs, 3.3% Rel

This value represents the at-sensor radiance uncertainty for a single target in a single image. Adding more targets in the scene will, in principle, reduce the net uncertainty and improve the performance knowledge of the sensor.

# Sensor Target Radiance Measurement Concept

- The goal is to measure from the L8 image data, the energy reflected only by the SPARC mirror target reaching the sensor.
- Since the target is subpixel, the energy distribution on the focal plane can be modeled by the sensor PSF
- Assuming that the area of the SPARC target surface is negligible, each target pixel contains a background radiance, that defines zero target signal floor
- Thus, placing the target on a uniform background much larger than the width of the central PSF profile allows the SPARC signal to be isolated by simple background subtraction, with a background radiance estimated from perimeter pixels.



Signal from specular target

Signal from background surface, sky path radiance, adjacency effect, stray light, etc.

# Extracting The Target Landsat Measured Radiance

- Convert the L1R product to radiance,  $L$  ( $W/(m^2 \text{ sr } \mu m)$ )
- From the channel,  $\lambda$ , integrate the total  $L$  response within a window of  $P$  pixels around each target image (image below shows  $P = 9$ ).
- Estimate an average background /pixel,  $\overline{L_{BG}}(S, \lambda)$ , for each target  $S$  calculated from pixels outside the perimeter of the target pixel window and subtract from each pixel ( $p$ ) before integrating.
- The integrated response to the SPARC target signal is than

$$\sum L_S(S, \lambda, X) = \frac{1}{Ens} \sum_{p=1}^P [L_S(p, S, \lambda, X) - \overline{L_{BG}}(S, \lambda, X)]$$

- The parameter  $Ens$  is the Ensquared Energy factor that corrects for the target energy outside the integration target area.

L8 Red Band Displayed by ENVI

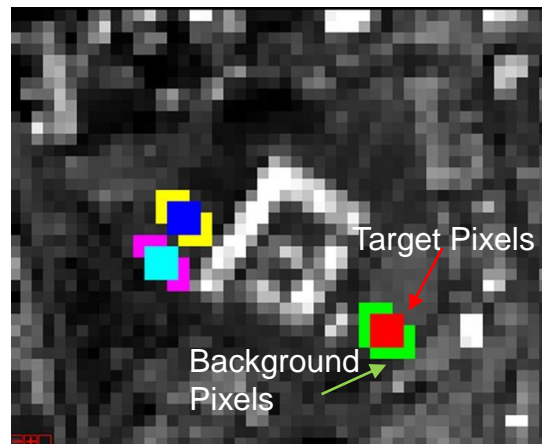
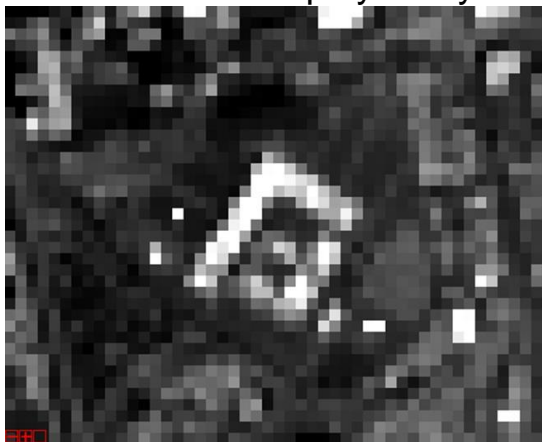


Image shows target and background regions- of-interest (ROIs) for measuring integrated radiance from calibrated L1R data. ENVI calculates the stats for each ROI.

# Estimated Uncertainty In The Landsat Image SPARC Target Radiance Measurement

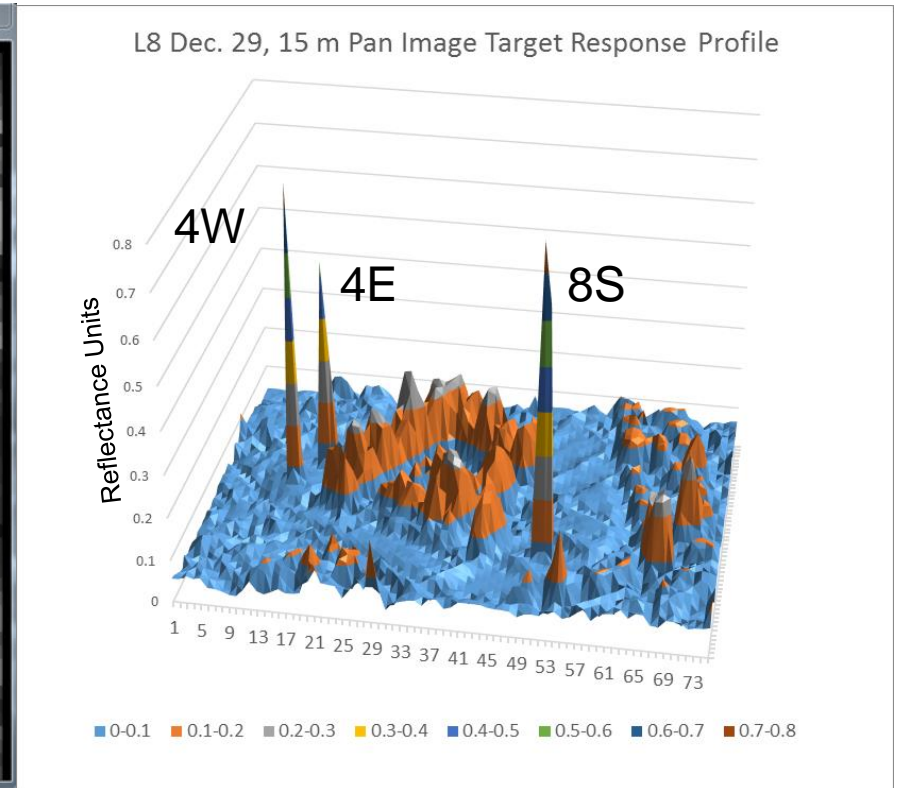
Based the SPARC target image analysis procedure, the estimated RSS uncertainty in the Landsat reported radiance for a single SPARC target is

$$\frac{\delta L}{L} [Landsat] = \sqrt{\left(\frac{\delta Ens}{Ens}\right)^2 + \left(\frac{\delta L_s}{L_s} + \frac{\delta \overline{L_{BG}}}{\overline{L_{BG}}}\right)^2} \quad (\text{based on } L_s > \overline{L_{BG}})$$

Symbol	Parameter	% Uncertainty
$Ens$	Ensquared Energy Correction Factor	1.0%
$L_s$	Landsat Measured Radiance of a SPARC Target Pixel Based On S/N	0.5% (Relative)
$\overline{L_{BG}}$	Average Estimated Background Radiance	2.0%
$L (Landsat)$	Landsat Reported At-Sensor Radiance of a SPARC Target	RSS total = 2.7% Rel

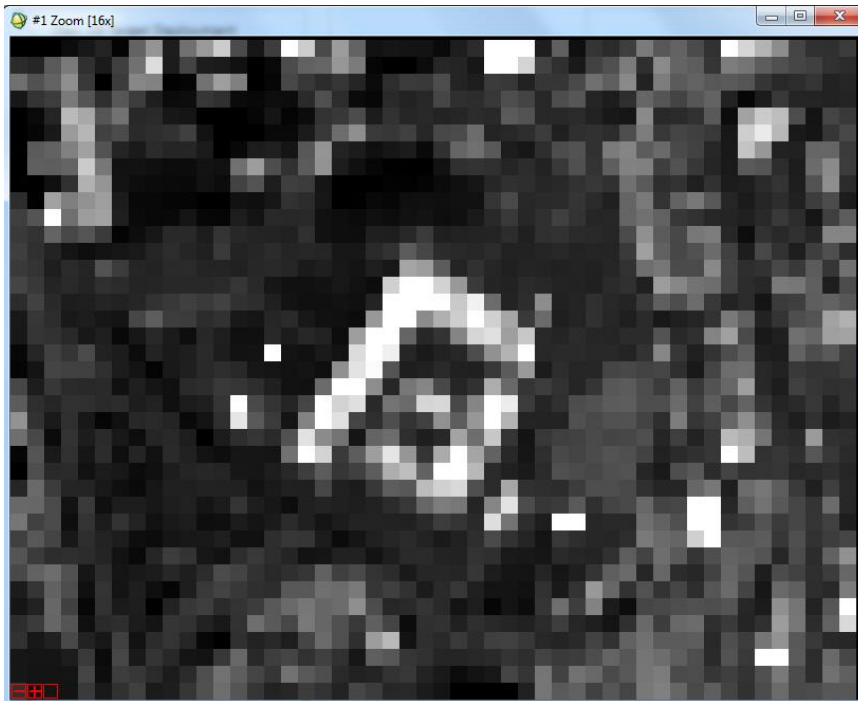
This value represents the at-sensor radiance uncertainty for a single target in a single image.

# L8 Pan Image SPARC target Response

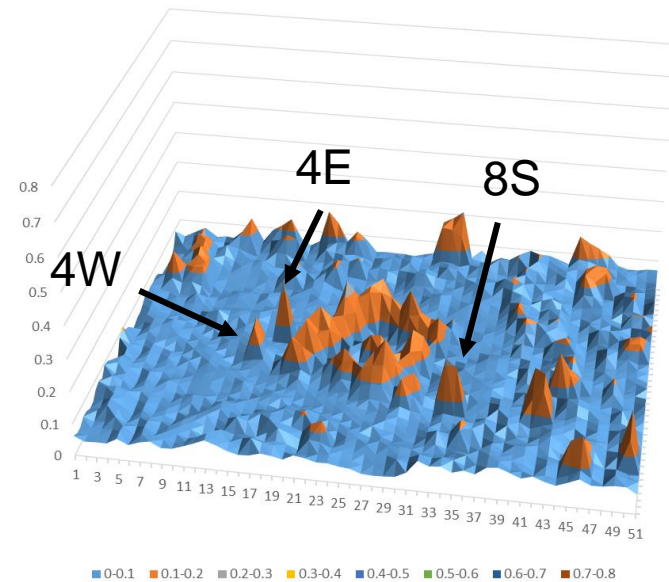


3D plot shows the relative brightness of the mirror targets compared to the rest of the scene. The central pixel response to target 8S is equivalent to a top-of-atmosphere Lambertian diffuse reflector of about 80% reflectance.

# Dec. 29 L8 Green Multispectral Band



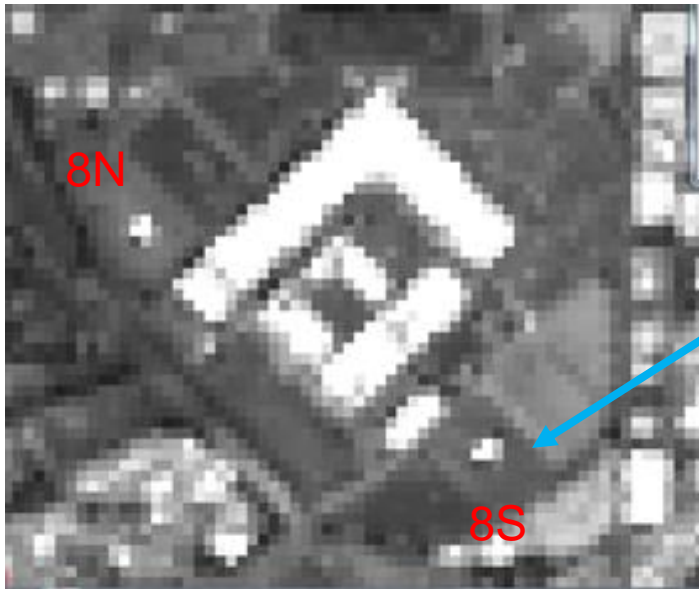
L8 Dec. 29, 30 m Green Band Image Target Response Profile



Acting as point targets, the multispectral bands response is much less than the Pan Band. Doubling the GSD from 15 m to 30 m decreases the integrated response by a factor of 4. The result is a response for the S8 target equivalent to a 20% Lambertian diffuser

## Feb. 15, 2016 Target Deployment

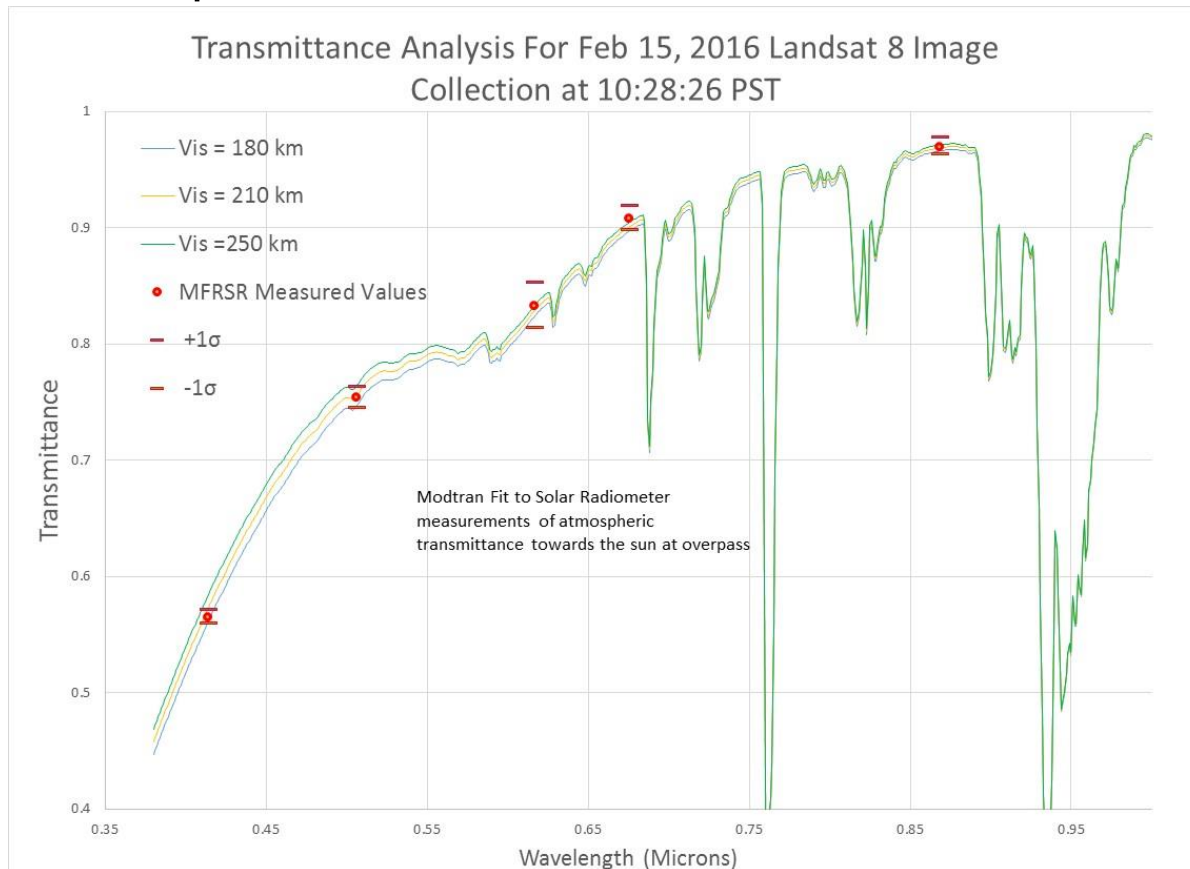
- Two identical mirror targets were set up 400 m apart in the El Segundo Parking lot (labeled 8N and 8S)
- Each target consisted of two aligned panels containing a total of 8 mirrors



- The Feb. 15 pan image above shows the location of the two targets

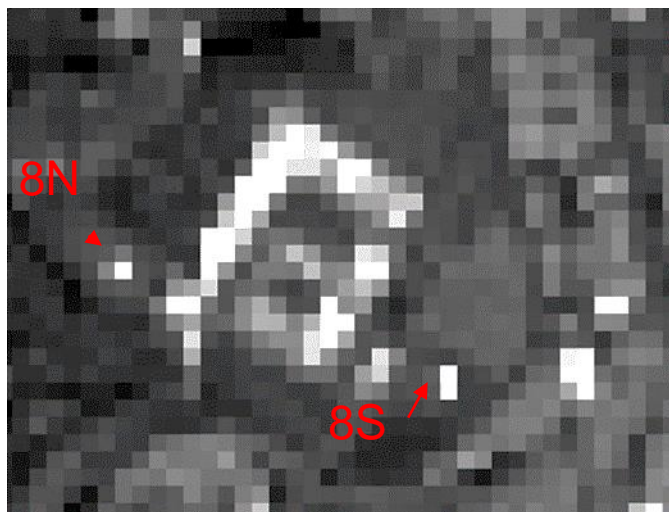
# Sky conditions On Feb. 15 Were Nearly Ideal At Overpass

- Minimal aerosol loading indicated by a best fit at a Visibility setting of VIS = 210 km and relative humidity at only 25%.
- Temperature was 85°F and no surface wind



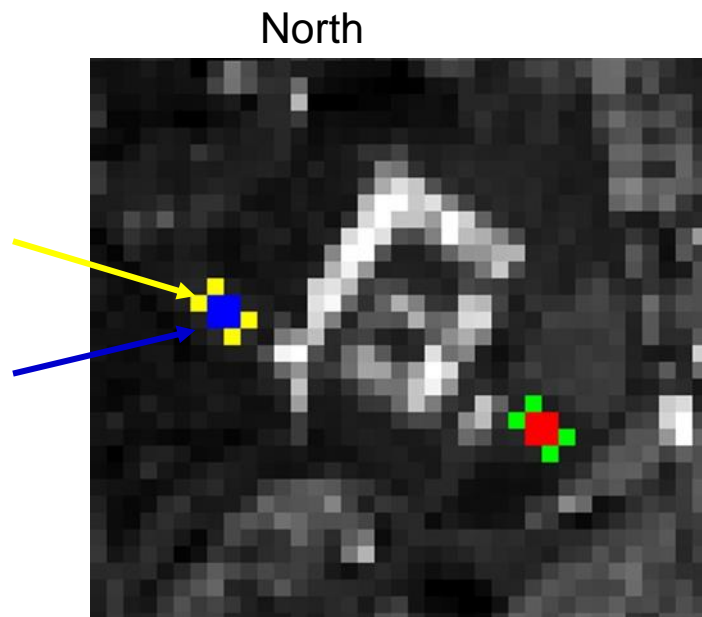
# Integrated Radiance Measurements

- The following images show the ROI placement used to calculate the integrated radiance from the L8 green band image.
- For each 2x2 pixel target area, the subpixel centroid was located and the pixel phasing offset applied to improve the ensquared energy correction estimate.



Background Pixels

Target Ensquared  
energy 2x2 pixel  
windows



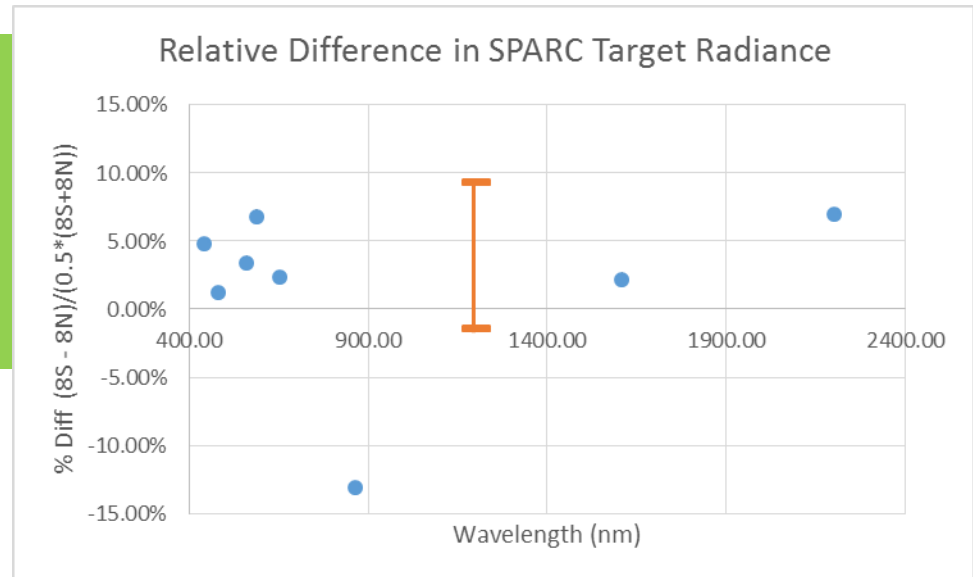
# Target Radiometric Repeatability For The Feb. 15 8N and 8S SPARC Reference Sources

- The following table and plot compares the L8 measured radiance between two equivalent SPARC targets, [% Diff  $(8S-8N)/(0.5*(8S+8N))$ ],
- The  $1\sigma$  uncertainty difference is estimated to be  $\sim 5.4\%$  (orange error bar)

L8 Spectral Band	CA	Blue	Green	Red	NIR	SWIR1	SWIR2	Pan
Band Center (nm)	442.90	482.00	561.40	654.60	864.70	1608.90	2200.70	589.50
8S Measured From Image ( $W/m^2 sr um$ )	225.12	255.10	279.66	266.22	153.67	44.37	14.84	268.81
8N Measured from Image ( $W/m^2 sr um$ )	214.86	252.03	270.40	260.15	176.83	43.41	13.87	251.63
% Diff $(8S - 8N)/(0.5*(8S+8N))$	<b>4.78%</b>	<b>1.22%</b>	<b>3.43%</b>	<b>2.33%</b>	<b>-13.09%</b>	<b>2.21%</b>	<b>6.99%</b>	<b>6.82%</b>

Except for the NIR band, all channels measure a difference within the estimated uncertainty

The NIR outlier appears to be a non-uniform energy-on-detector response issue for the detectors containing the target image centroid



A bias of about 4% between the two targets is indicated and may be the result of the limited statistics from the small sample size.

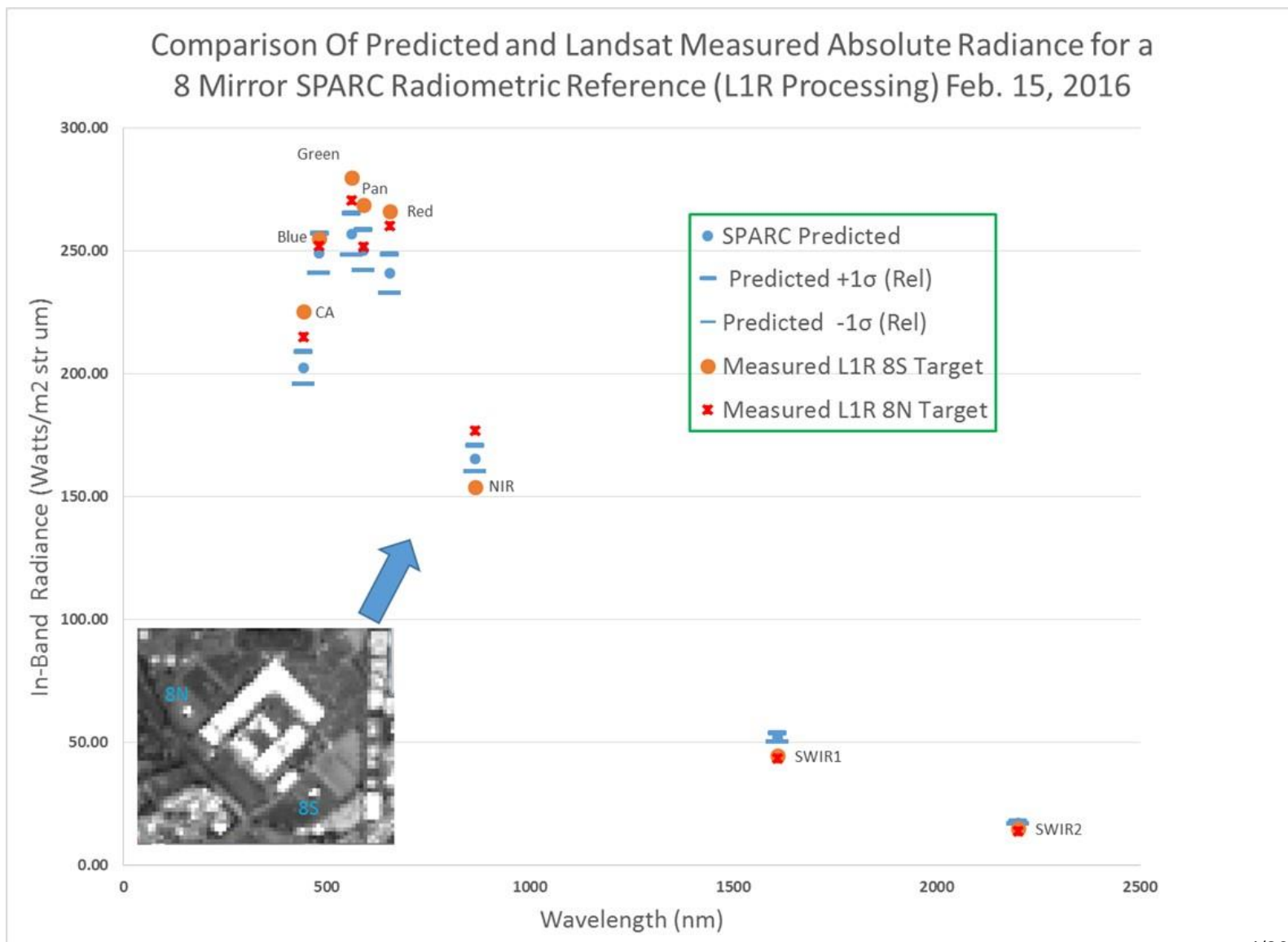
# Absolute Radiance Comparison Between SPARC Predicted and L8 Measured Radiance

- The following table presents the difference between the L8 measured radiance and the SPARC vicarious predicted radiance, [%Diff (vicarious-L8)/L8], for the Feb 15 collect.
- Based on the estimated uncertainties in the two quantities, the  $1\sigma$  difference should be  $\sim 6.0\%$

L8 Spectral Band	CA	Blue	Green	Red	NIR	SWIR1	SWIR2	Pan
Band Center (nm)	442.90	482.00	561.40	654.60	864.70	1608.90	2200.70	589.50
Predicted SPARC Radiance (Vicarious)	202.37	248.95	256.63	240.68	165.43	51.80	17.11	250.25
Mean 8N and 8S L8 measured Radiance (L8)	219.99	253.56	275.03	263.19	165.23	43.89	14.35	260.22
%Diff (vicarious-L8)/L8	-8.01%	-1.82%	-6.69%	-8.55%	0.12%	18.02%	19.17%	-3.83%

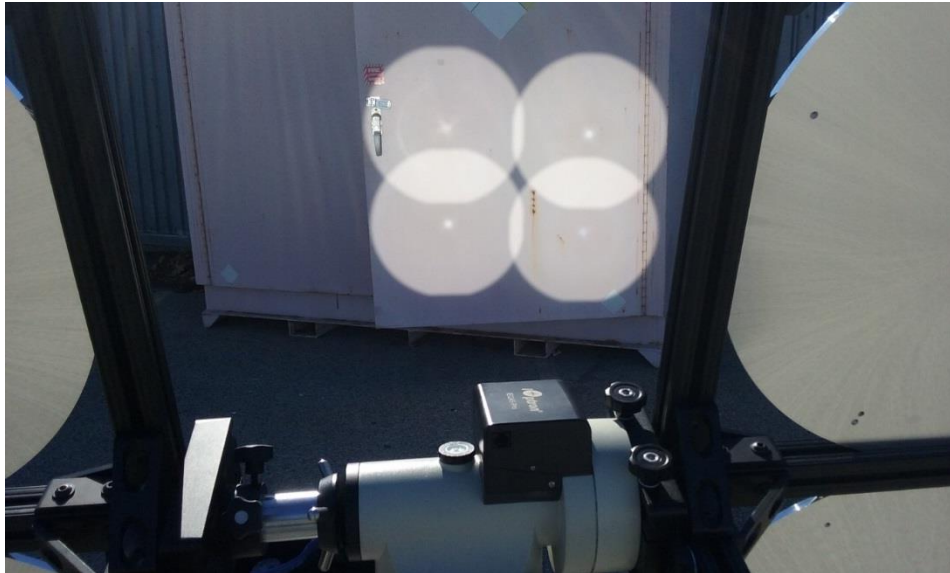
- The results show that the measured radiance difference in the VNIR bands is consistent with the predicted uncertainties.  
(VNIR L8 measured bias  $\sim 5\%$  higher than predicted – likely due to scattered light issue from the diamond turned mirror construction)
- The difference in the SWIR bands is likely from the targets being recorded at the edge of the upwelling uniform field-of-regard (FOR) where the target intensity is starting to drop.  
(SWIR bands are the first or last bands to see the targets based on focal plane layout and indicates the need for better centering of FOR on L8 position when imaging targets)

# Radiance Analysis Results for Feb 15, 2016 Collect



# Description Of Field-of-Regard Radiometric Illumination Bias By Diamond Turned Mirrors

- An intensity bias from a non-uniformity in the mirror projected field-of-regard (FOR) was identified



Mirror reflected solar flux projected onto a white surface shows significant non- uniformity at the center of the FOR (near field)

Likely caused by a mirror scattering asymmetry due to the axial rotation of the diamond turning process producing a “Fresnel lens” like effect focusing scattered light like a positive lens along central mirror axis into the upwelling field-of-regard.



Illustration only: not one of the SPARC mirrors  
4/26/2016

# Diamond Turned Groves Are Creating A Positive At The Mirror Center

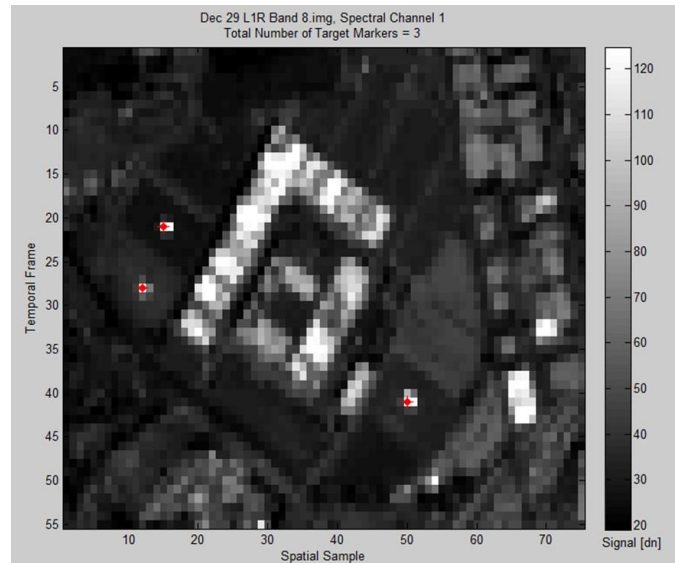
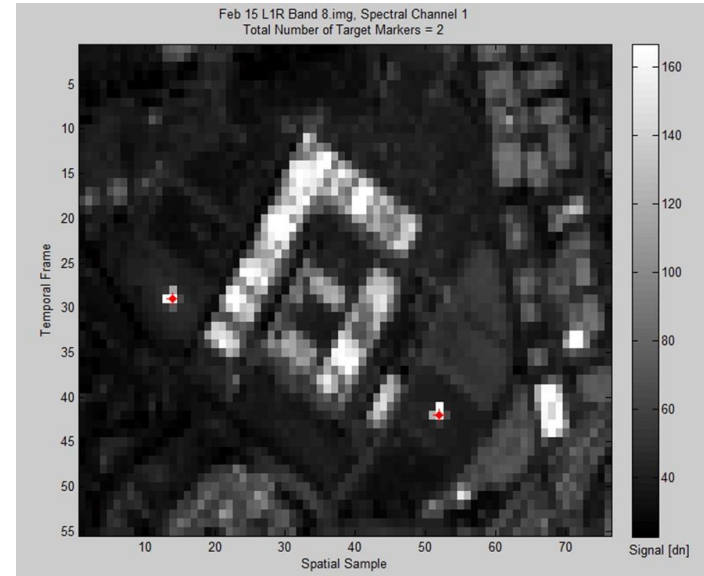
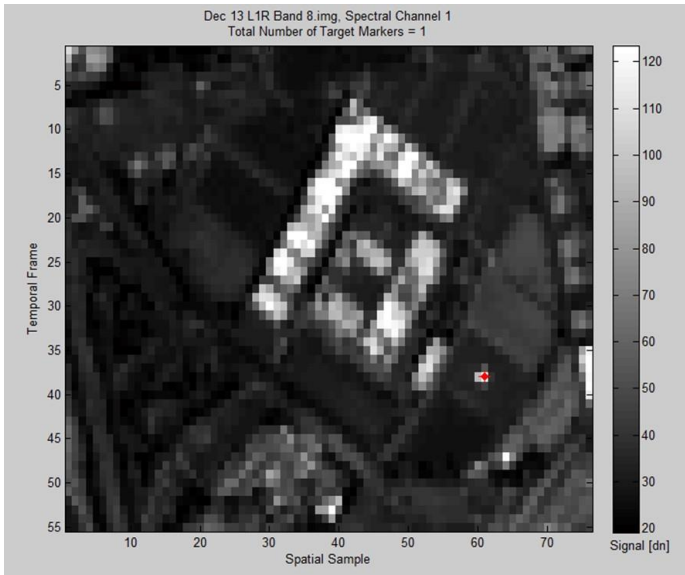
- Blocking the reflected light through the center of the mirror shows that the center bright spot is persistent and coming from light focused by entire mirror.



A strip is placed across the mirror to block light reaching the mirror surface.

- Note the blue color of the scattering bright spot indicating the magnitude of the scattering effect is wavelength dependent as expected if caused by diffraction grating like effect
- Moving the mirror closer or away from the screen causes the center spot to become shaper or widen with focal length of 4 meters or more.
- The result is to increase the upwelling intensity within the FOR making the mirror target brighter than predicted.

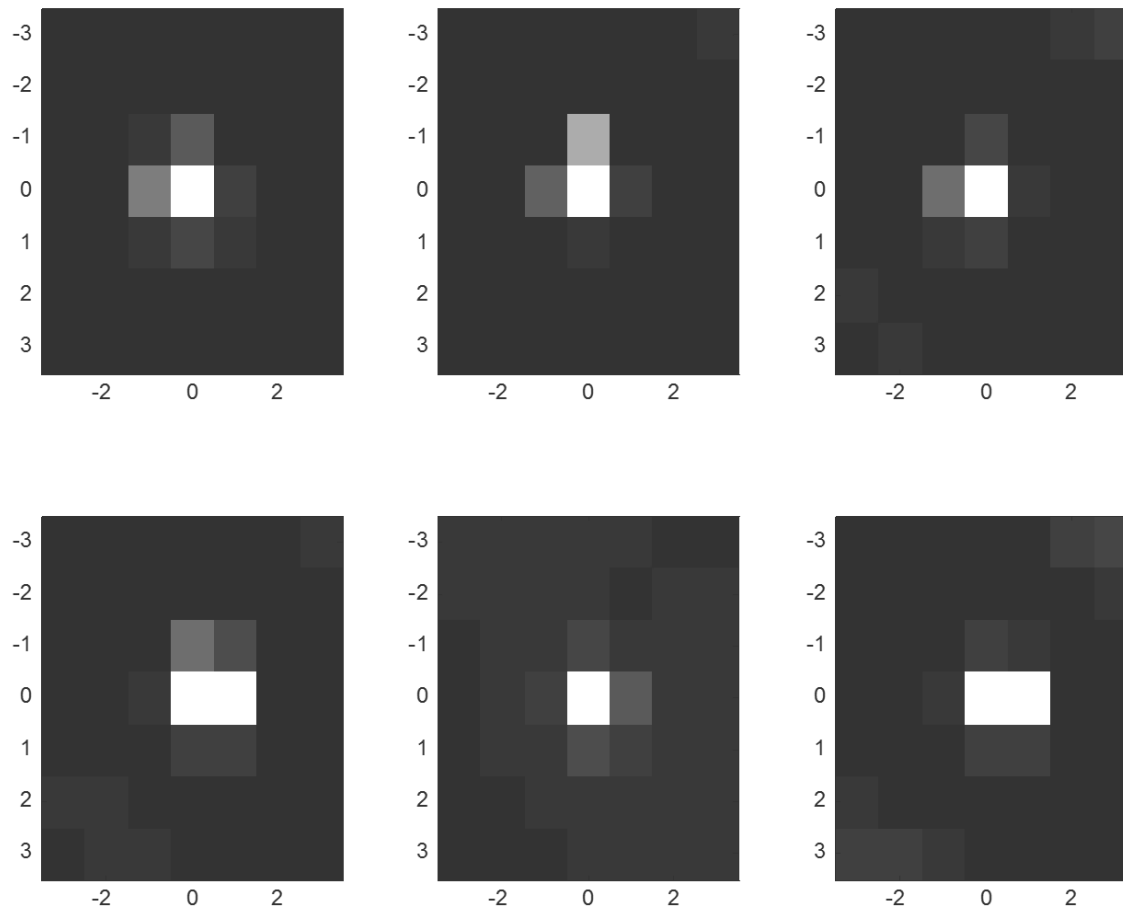
# Landsat 8 Panchromatic PSF Analysis



Data from three L8 collects available for analysis.

Random target positions provide variation in pixel phasing for oversampling the system level PSF

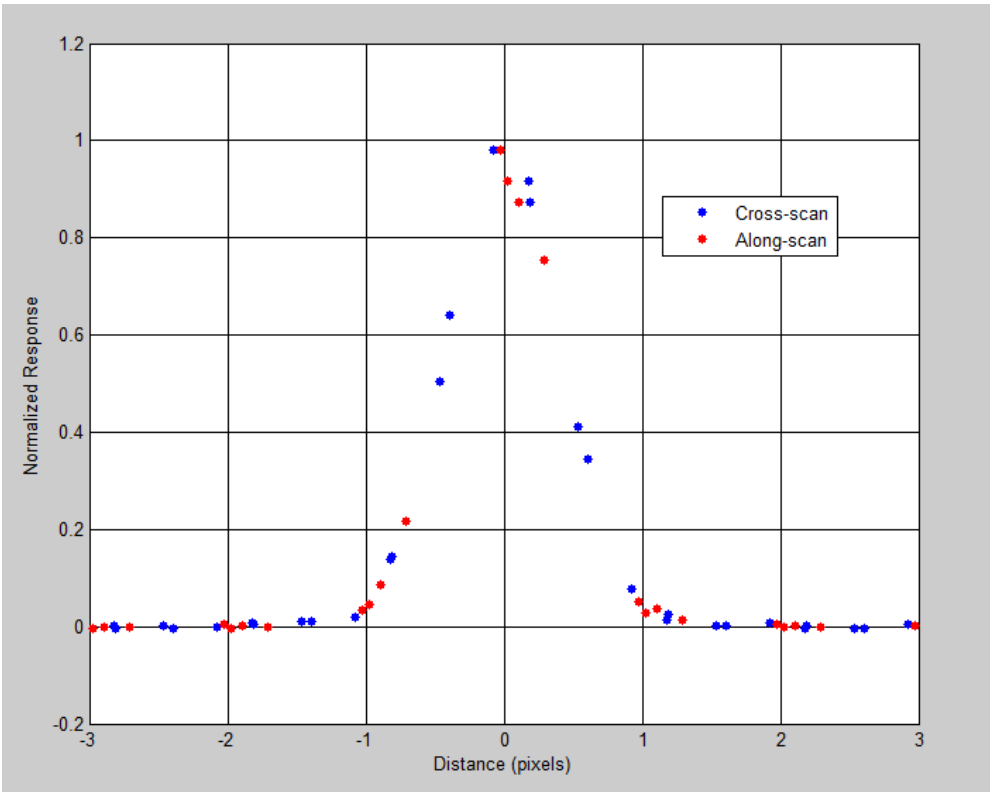
# SPARC Target Images For Oversampling PSF



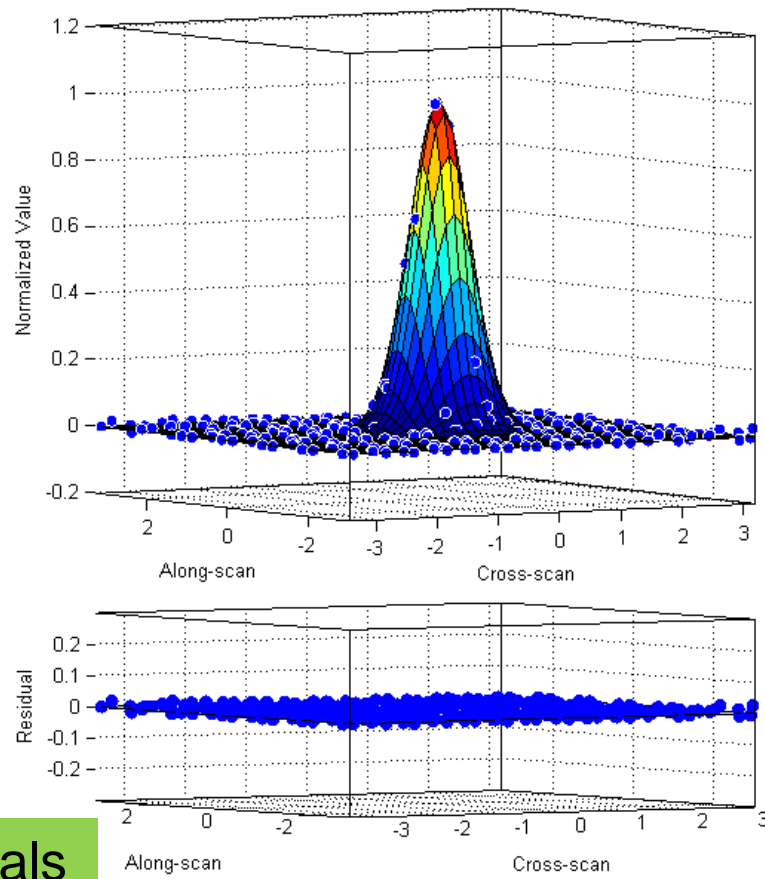
Each 7 x7 pixel image (15 m GSD) is fit with a Gaussian profile using regression analysis to locate individual centroids and align to a common center to produce the composite oversampled 2D PSF profile.

# Sensor System Composite 2D PSF Profile For L8 Pan Band

Cross-scan and along-scan slices through the composite profile center



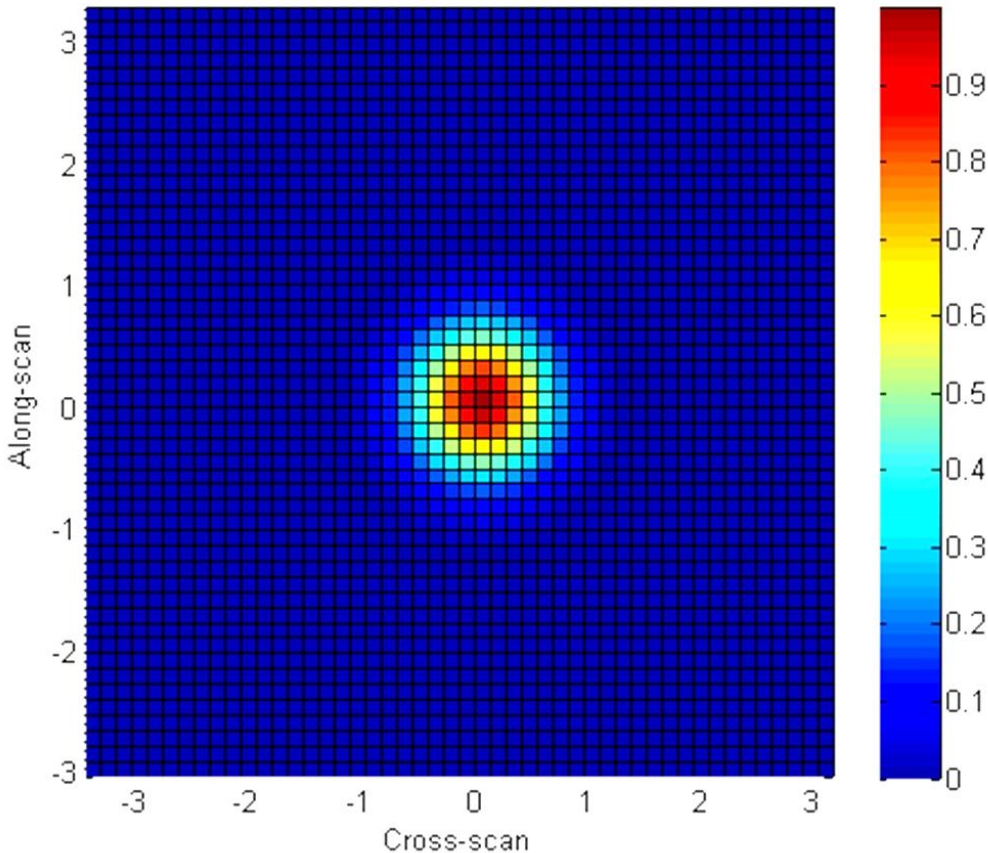
Composite 2D PSF Profile Residuals show no outliers



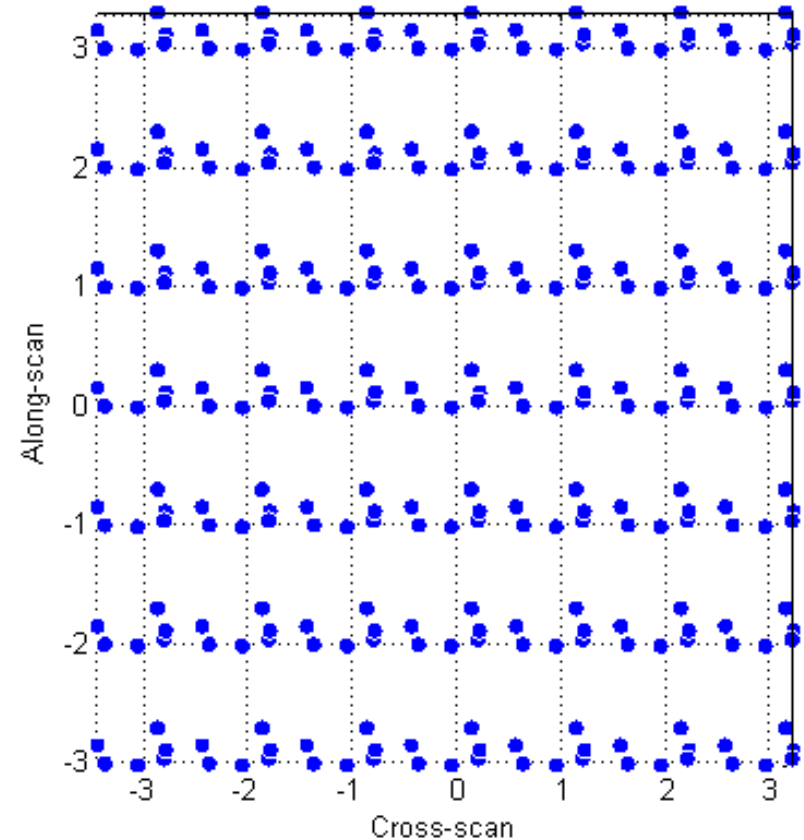
System level PSF shows negligible residuals when modeled as a Gaussian function.

# Top View Of Composite Gaussian Model

Top view spatial profile



Composite pixel sampling points after alignment of individual profiles centroids to a common center

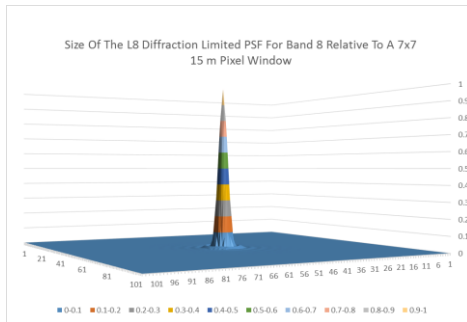


Symmetric profile indicates that along-scan integration smear is not significant.

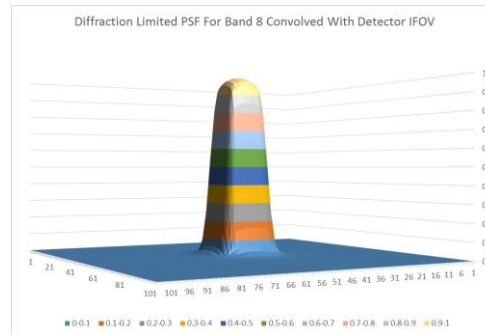
# Statistics and Parameters From The Gaussian Model Fit To the Landsat 8 Pan Band Oversampled System PSF

	PSF FWHM (Pixels, 15 m)	Goodness of Fit $R^2$	MTF @ Nyquist	Relative Edge Response
Cross-Scan	$0.977 \pm 0.003$	0.9978	0.4275	0.7718
Along-Scan	$0.959 \pm 0.005$	0.9978	0.4411	0.7840

## System Level PSF Formation Process



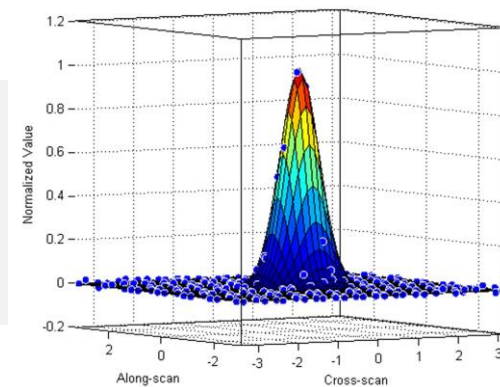
Diffraction PSF



Convolved with square detector IFOV response

Wave Front Error  
Jitter  
Spacecraft Motion  
Detector Integration  
...

Convolved with other PSF effects



SPARC measured system level PSF

**Central limit theorem is alive and well.**

# Results Summary

- This paper reports on the first demonstration of SPARC vicarious radiometric calibration applied to Landsat 8.
- Targets achieved operational efficiency by being highly portable, robust and easy to deploy – demonstrated a single person deployment capability
- Predicted performance of the SPARC method with actual target properties and site conditions, established that a single subpixel target is capable of providing a vicarious radiometric reference with an absolute accuracy knowledge of  $\sim 4.3\%$  and a repeatability between targets of  $\sim 3.3\%$  when deployed at sea level – multiple target observations can result in better statistics for achieving less than  $3\%$  absolute accuracy knowledge.
- Within measurement uncertainties, except for one outlier at 865 nm, the results confirmed the predicted target relative repeatability over the full L8 spectral range
  - More work is needed to understand impact of possible pixel response non-uniformity on repeatability
- Absolute radiance comparison showed a possible bias (up to  $\sim 5\%$ ) in the VNIR SPARC L8 measured radiance that is probably caused by light scattering artifacts resulting from the diamond turned construction of the SPARC mirrors
  - Further analysis and design adjustments are planned to resolve this issue.
- An oversampled 2D system level PSF was successfully derived for the panchromatic band from the SPARC target point source images revealing a profile modeled accurately by a Gaussian function.

# Conclusion

---

- As demonstrated, the SPARC method has the unique capability of assessing both sensor radiometric and image quality performance making it the only comprehensive in-scene vicarious approach for addressing issues of small target radiometry.
- The next step is to work with mirror manufacturers finding a cost effective solution to improving the mirror FOR uniformity and expand the analysis statistics with more Landsat and Sentinel-2 collects.
- It is anticipated that collections will continue this summer with the potential to set up SPARC targets in conjunction with reflectance-based field campaigns.
- Though applying SPARC at Landsat spatial resolutions is revealing some challenges in this initial study, there are no showstoppers. With continued testing and modifications, it is anticipated that the SPARC method will achieve the <3% absolute repeatability already demonstrated with small spatial resolution sensors.